

**Equation-of-motion method for the study of defects in insulators:
Application to a simple model of TiO₂**

J. W. Halley

School of Physics and Astronomy, University of Minnesota, Minneapolis, Minnesota 55455

Herbert B. Shore

Department of Physics, San Diego State University, San Diego, California 92182

(Received 26 November 1986; revised manuscript received 16 April 1987)

We illustrate the advantages of an equation of motion technique for calculation of the electronic structure of oxides. The technique is described in some detail and applied to a simplified version of a tight-binding model of TiO₂ due to Vos. We can determine the density of states of systems with arbitrary numbers of oxygen vacancies in this model with very modest expenditures of computer time. We discuss some physical implications of the results.

INTRODUCTION

Defects play an essential role in many models for the passivation layer. As an example we recall the model of Chao, Lin, and MacDonald¹ in which oxygen vacancies, metal vacancies, electrons, and holes all play a role in the processes leading to film growth. In the case of TiO₂, for example, the literature suggests² that oxygen vacancies and Ti³⁺ interstitials may be among the important defects in the system. To make meaningful microscopic theories of the passivation film formation process, it is essential to know the nature of the defects in more detail. Unfortunately, it has not been practical to obtain theoretical information about more than one defect in an oxide using conventional techniques which make use of the periodicity of the defect-free lattice. (In fact, using conventional Koster-Slater techniques,³ even the calculation of the electronic structure of one defect is a formidable task.⁴) In the present paper we describe the use of the equation of motion technique for studying multiple defects in oxides.⁵ We show that the electronic structure of essentially arbitrary configurations of defects can be obtained quite easily in this way. To illustrate, we present results on single vacancies and random collections of vacancies.

In the next section we review the equation of motion method and describe how we have improved it for use in these problems. The third section describes the model of TiO₂, and gives results. The last section contains a discussion and conclusions.

**EQUATION OF MOTION METHOD
FOR A TIGHT-BINDING
ELECTRONIC STRUCTURE**

The basic approach of the equation of motion method is⁵ to solve the time-dependent Schrödinger equation

$$i\hbar\partial\Psi/\partial t = H\Psi,$$

and then to Fourier transform the result in time to obtain the quantities such as the density of states which are

of interest at the end of the calculation. We work with a tight-binding Hamiltonian

$$H = \sum_i \epsilon_i c_i^\dagger c_i + \sum_{(i,j)} (t_{ij} c_i^\dagger c_j + \text{H.c.}).$$

Here the *i*'s are site indices and the sum on (*i,j*) is over neighbors on the lattice. We define a Green's function

$$G_{ij}(t) = -i\Theta(t)\langle\{c_i(t), c_j^\dagger(0)\}\rangle$$

and an amplitude

$$F_i(t) = \sum_j a_j G_{ij}(t).$$

The amplitudes *a_j* can be chosen in various ways depending on what quantity is of particular interest. The equation of motion for *F_i* is

$$i\hbar\partial F_i/\partial t = \sum_j H_{ij} F_j,$$

with initial condition

$$F_i(0) = -ia_i.$$

For example, we get a global approximation to the density of states *N*(ω) defined as

$$N(\omega) = \sum_n \delta(\omega - \epsilon_n)$$

by setting

$$a_i = e^{i\phi_i},$$

where ϕ_i is a number chosen for each site at random from the interval $0 < \phi_i < 2\pi$. The density of states is then

$$N(\omega) = -\frac{1}{\pi} \text{Im} \left[\int \sum_i e^{-i\phi_i} F_i(t) e^{-i\omega t} dt \right].$$

To get the local density of states, defined as

$$N_k(\omega) = \sum_n |\langle k | n \rangle|^2 \delta(\omega - \epsilon_n),$$

we set

$$a_i = -i\delta_{i,k} ,$$

where k is the site of interest. In these expressions, n denotes an eigenstate of the Hamiltonian and i, j , and k refer to states in the tight-binding basis. $\langle k | n \rangle$ is the coefficient multiplying the wave function of tight-binding orbital k in an expansion of the exact eigenstates n in terms of these tight-binding orbitals. Thus the local density of states $N_k(\omega)$ provides information about the spatial extent of the wave function associated with a given energy.

The equation of motion method is closely related to another well-known sparse matrix method, the recursion method.⁶ A critical discussion of the two methods appears in Ref. 7. The methods are of roughly equal efficiency but the equation of motion method has the advantage that it can be manipulated to limit the calculational effort only to those quantities of particular experimental interest.

Our successful numerical implementation of the equation of motion method depends on our algorithm for the integration of the equation of motion forward in time. The equation of motion method must be integrated to produce a time sequence $F_i(t_l)$ at a discrete set of time t_l . F_i is a vector with a number of components equal to the size of the system. At each time step l , we produce and save a single number $F(t_l)$ according to the prescription

$$F(t_l) = \sum_i e^{-i\phi_i} F_i(t_l)$$

if we are calculating the total density of states, or

$$F(t_l) = F_k(t_l)$$

if we are calculating the local density of states at site k . We obtain the spectral density from $F(t_l)$ using the fast Fourier transform; thus we require F at discrete times $t_l = (l-1)\delta t$, $l=1, \dots, N_w$, where we use $N_w = 256$. The time interval δt is determined by the bandwidth ω_0 of the output spectrum. The diagonal elements of the Hamiltonian are shifted by a constant value in order to center the spectrum around $\omega=0$. The spectrum then extends from $-\omega_0/2 \leq \omega \leq \omega_0/2$; thus $\delta t = 2\pi/\omega_0$. It is important that ω_0 be chosen large enough to encompass the entire spectrum of H_{ij} to prevent aliasing. The sequence $F(t_l)$ is multiplied by a Gaussian window

$$\exp \left[-\alpha \left(\frac{l-1}{N_w} \right)^2 \right] .$$

We use $\alpha=8$. The point at $l=1$ is multiplied by 0.5 to account for the step function in time.

In solving the equation

$$i\hbar dF_i/dt = \sum_j H_{ij} F_j ,$$

we have the unusual situation that we need the solution at discrete times t_l . This differs from the usual case where we try to make the time step as large as possible. We can then exploit the exact formal solution

$$F(t_{l+1}) = \exp(\underline{H}\delta t)F(t_l)$$

by using a polynomial approximation $P(\underline{H}\delta t)$ to the exponential. Because the spectrum of \underline{H} contains energies $|\omega| \leq \omega_0/2$ and $\omega_0\delta t = 2\pi$, the $P(x)$ must be a good approximation to $\exp(ix)$ over the interval $-\pi \leq x \leq \pi$. We use a tenth-order Taylor expansion, resulting in ten multiplications by \underline{H} per time step. Since the range of x is limited, the Taylor expansion is far from optimal; for example, a considerable reduction in the number of multiplications could be obtained using, for example, an expansion in Chebyshev polynomials.

RESULTS ON A SIMPLE MODEL OF TiO₂

To illustrate the power of the method for this type of problem, we have formulated a simplified tight binding-model of a layer of TiO₂ which is designed to take the essential features of its structure into account. As discussed below, we find that most of the qualitative

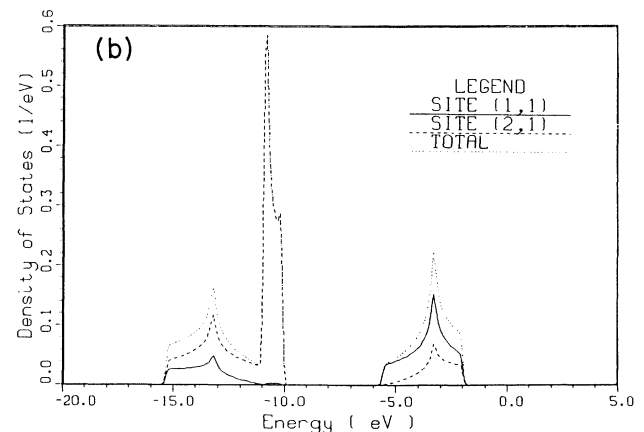
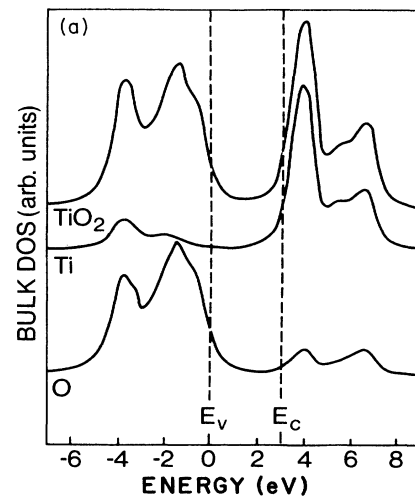


FIG. 1. (a) Density of states of the full Vos model for bulk TiO₂ (from Ref. 9). (b) Density of states for the simplified model using the equation of motion method and the model for a two-layer film shown in Fig. 2.

features of the band structure are reproduced by a model in which there is only one orbital per site. We use the following values of the parameters, suggested by a more complete tight-binding model of Vos⁸ for the band structure of defect-free rutile: (the quantities t_1 , t_2 , and t_3 are off-diagonal matrix element defined in Fig. 2)

$$\begin{aligned}\epsilon_{\text{Ti}} &= -6.4 \text{ eV} , \\ \epsilon_{\text{O}} &= -10.5 \text{ eV} , \\ t_1 &= -2.3 \text{ eV} , \\ t_2 &= -0.2 \text{ eV} , \\ t_3 &= 0.4 \text{ eV} .\end{aligned}$$

We find that this simplified model gives a fairly good representation of the TiO_2 density of states as indicated in Fig. 1, where for reference we also indicate the full density of states as calculated by Munnix and Schmeits⁹ from the Vos model. (The agreement is somewhat better than might be suggested by Fig. 1 because the authors of Ref. 9 have broadened their calculated results by convoluting them with a Lorentzian of width 0.3 eV.) In the calculations leading to the density of states shown in Fig. 1, we performed the equation of motion calculation on a model of TiO_2 consisting of two layers of TiO_2 with faces in the 100 direction as indicated in Fig. 2. The model contained 576 formula units of TiO_2 or 2304 Ti sites and 4608 O sites. The calculations giving the results of Fig. 1 as well as those reported on defects below took about 30 sec of CPU time on the Cray-2. One sees

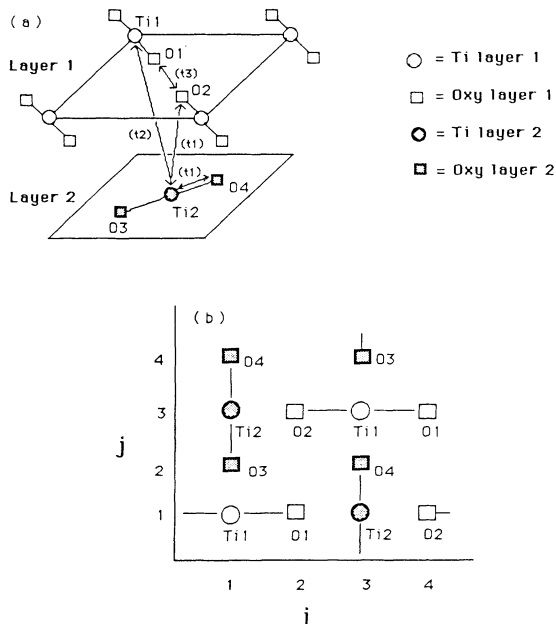


FIG. 2. (a) Rutile structure of TiO_2 showing the off-diagonal matrix elements t_1 , t_2 , and t_3 used in our model. (b) Two layers of TiO_2 as used in the calculations reported here with definitions of site indices (i, j) .

from Fig. 1 that the main qualitative and semiquantitative features of the density of states are reproduced in the simpler model. The most important feature is the existence of a gap separating valence and conduction bands. The semiconductor is highly ionic, with the valence states residing primarily on O^{2-} sites and (unoccupied) conduction-band states primarily on Ti^{4+} sites. This partitioning of the density of states is also displayed in Fig. 1 by a decomposition of the total density of states into two components associated with the local density of states on the titanium and oxygen sites. A peak associated with the density of t_{2g} symmetry d states in the conduction band is not reproduced. The states left out are highly localized on the Ti ion; thus we believe that these states are unlikely to play a significant role in defect electronic structure. The gap which we calculate in our simplified model is larger (4.1 eV) than the band gap of the full model (3.04 eV).

A completely microscopic model of the electronic structure of defects in TiO_2 requires a fully self-consistent Hartree-Fock or local-density-approximation type of calculation, which we will not undertake here.¹⁰ One model, used by Munnix and Schmeits⁴ for oxygen vacancies on the surface of TiO_2 , suggests that the essential features of the electronic structure of the defect are sufficiently described by a model in which there is a very large repulsive barrier for the electron to be on the vacancy site (corresponding in our tight-binding model to a very large positive value of the diagonal matrix element there). We have explored such a model numerically using the equation of motion methods and find that it results in no donor state in the band gap, in agreement with a calculation of Munnix and Schmeits.⁴ These authors attribute an observed¹¹ donor state to a surface vacancy. On the other hand, there is much experimental evidence¹² from the temperature-dependence of conductivity and infrared absorption of reduced TiO_2 (Ref. 10) that oxygen vacancies do result in donor levels in the bulk. Furthermore, we expect on physical grounds that

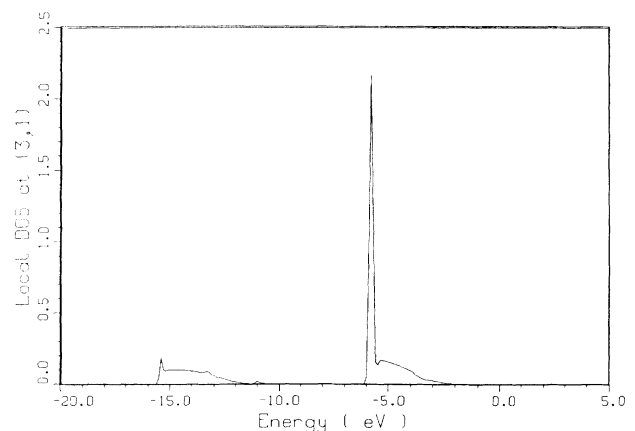


FIG. 3. Local density of states at the (3,1) position (next Ti neighbor of the vacancy) for our model of the oxygen vacancy at position (2,1).

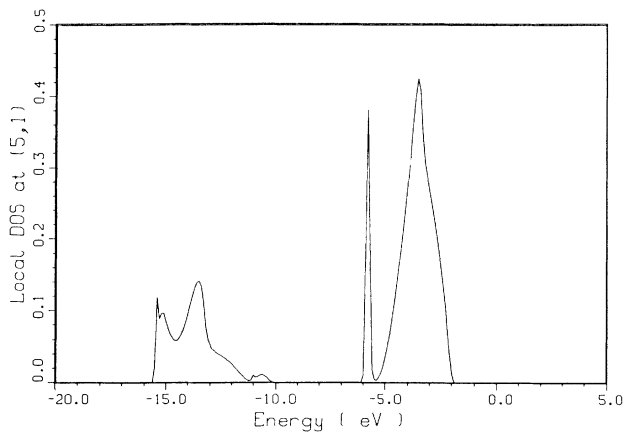


FIG. 4. Same as Fig. 3 but at the (5,1) Ti position, farther from the defect.

electrons will be attracted to a neutral oxygen vacancy by a screened Coulomb potential because the two electrons which must be added to the system to assure charge neutrality when an O^{2-} is removed from the system must be found in somewhat extended orbits in the vicinity of the vacancy.¹³ For these reasons we choose a model in which the oxygen vacancy is described in the tight-binding model by a modification of the tight-binding diagonal elements by an amount $Q \exp(-\beta r)/\epsilon_\infty r$ where r is the distance from the site in question to the vacancy site and β and Q are parameters. In addition we assume that the off-diagonal matrix elements V which couple states on the vacancy site to neighboring sites are all zero and that the diagonal matrix element on the site is zero (which is far above the conduction band). In the calculations reported below, we take $Q=2$ and $\beta=0.50 \text{ \AA}^{-1}$. These assumptions are qualitatively reasonable. We will see below that they lead to densities of states for the single defect which are

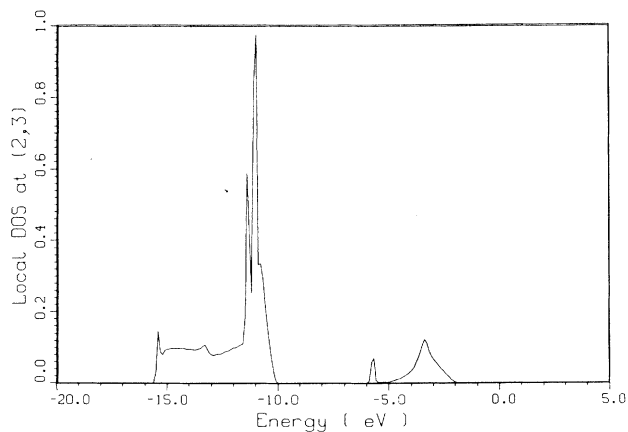


FIG. 5. Same as Figs. 3 and 4 but at oxygen position (2,3), showing that the defect wave function has small amplitude at the oxygen site.

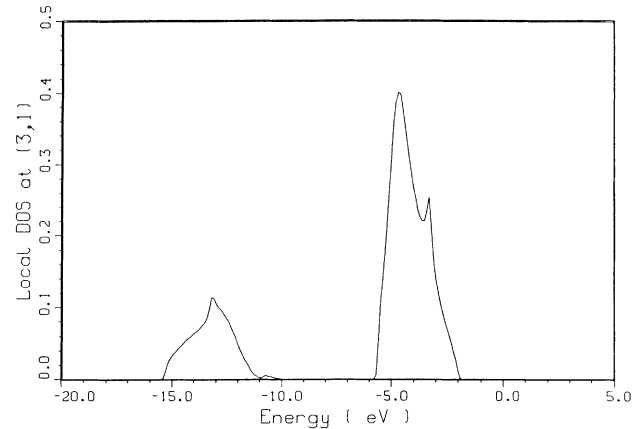


FIG. 6. Density of states for an oxygen vacancy in the model of Munnix and Schmeits (Ref. 4). The vacancy is at (2,1) and the density of states is evaluated at (3,1). This is to be compared with Fig. 3, showing our model of the defect. Here we took the diagonal matrix element at the oxygen vacancy site to be 2.0 eV and set all off-diagonal elements to the vacancy equal to zero.

in semiquantitative accord with experiment.

In Fig. 3 we show the density of states for a single oxygen vacancy using the model just described. This is the local density of states at the first-neighbor titanium site next to the oxygen vacancy. One sees that a clearly pronounced donor level has appeared a few tenths of an eV below the conduction band as observed in the conductivity and absorption experiment.¹⁰ In Figs. 4 and 5 we show the density of states in the same model at positions progressively farther away from the vacancy as defined in those figures with reference to the site labeling scheme defined in Fig. 2. It is clear that the donor level of the

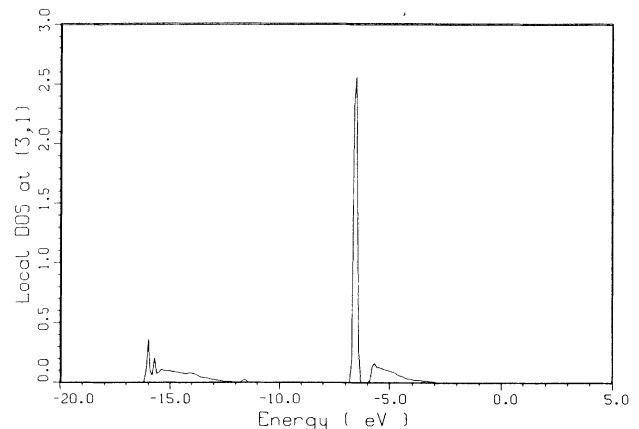


FIG. 7. Density of states for an oxygen vacancy in a model in which the defect is ionized. The diagonal elements at all the sites are modified by an amount $2|e|/r\epsilon_\infty$ where r is the distance to the defect. The defect and the point at which the local density of states is evaluated are the same as in Figs. 3 and 6.

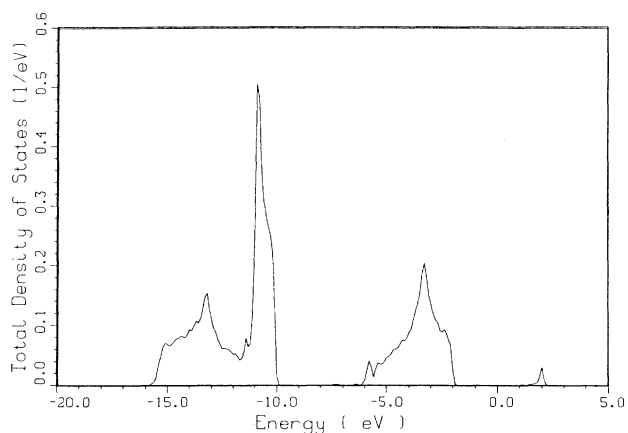


FIG. 8. Total density of states for 1% oxygen vacancies. The arrows show the position of the band edges (ϵ_v, ϵ_c) and the single-vacancy donor level ϵ_D .

single vacancy is bound to the vacancy. We have established that the donor state shown in these figures is doubly degenerate by showing that it can be split by introducing finite values of the matrix elements coupling the vacant oxygen site to its neighbors.

To contrast this model of the oxygen vacancy with that of Ref. 4 on the one hand, and with an ionized defect on the other, we have also computed the density of states for these two models of the defect. In Fig. 6 we show the density of states for a model in which the oxygen defect is modeled by making the diagonal matrix element at the oxygen site very large and making the off-diagonal elements to this site zero. This corresponds to the model of Ref. 4. In agreement with that reference, there is no donor state in the gap. Instead, there is a resonance in the conduction band arising from the vacancy. We note that, if such a resonance exists in the conduction band, then when the states are filled to the Fermi level the donor will be ionized. This means that in the next iteration of an electrostatically self-consistent calculation, the donor would appear as an unscreened charge of $+2|e|$ with potential $+2|e|/r\epsilon_\infty$. In Fig. 7 we

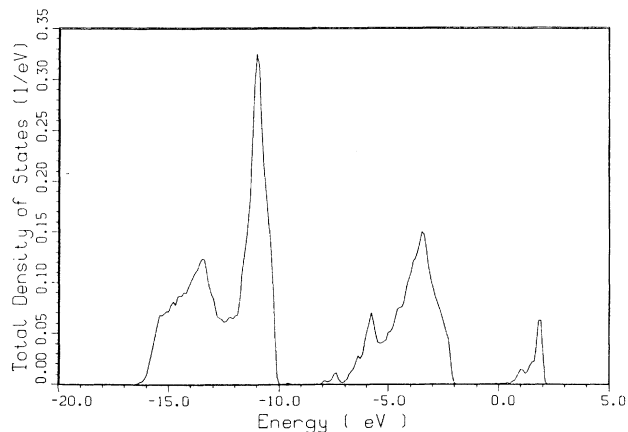


FIG. 9. Same as Fig. 8 for 5% vacancies.

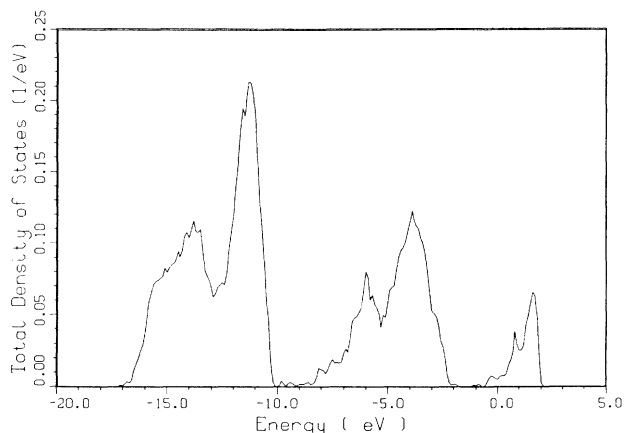


FIG. 10. Same as Figs. 8 and 9 for 10% vacancies.

show the results of computing the density of states for such a model of the defect. One sees that several bound states appear in the gap as a consequence of the large Coulomb attraction. Our model (Figs. 3, 4, and 5) lies between these two extremes.

In Figs. 8, 9, and 10 we show the result of adding increasing numbers of oxygen vacancies to the model. Here the vacancies were added to the model at random with probability $p=0.01, 0.05,$ and $0.1,$ respectively. One sees clearly that a band of donor levels develops and gradually tails into the gap as the number of vacancies increases. In these pictures, we note that far above the conduction band the impurity has resulted in another band of levels, corresponding to a localized electron in the vacancy itself, as in an F center in alkali halides. While our model cannot be expected to correctly predict the position of such states, it seems clear they ought to exist.

DISCUSSION AND CONCLUSIONS

These results indicate that the new methods employed can yield new information on the electronic structure of a system such as TiO_2 which can be described by a tight-binding Hamiltonian but which has large numbers of defects. Though our model is too simple to be fully realistic, we emphasize that no calculations with such large numbers of defects could even be attempted using earlier methods.

It is obviously important to extend the work reported here to a model of TiO_2 which includes a more complete basis of tight-binding states and to thicker films. Such calculations are completely feasible using the present methods, and are under way.

ACKNOWLEDGMENTS

This work was supported in part by the Corrosion Center at the University of Minnesota, U. S. Department of Energy Grant No. DOE/DE-FG02-84ER45173, and by a grant from the Supercomputer Institute of the University of Minnesota.

- ¹C. Y. Chao, L. Lin, and D. D. MacDonald, *J. Electrochem. Soc.* **128**, 1187 (1981); **128**, 1194 (1981); **128**, 1874 (1982).
- ²P. F. Chester, *J. Appl. Phys.* **32**, 2233 (1961).
- ³G. F. Koster and J. C. Slater, *Phys. Rev.* **95**, 1167 (1956).
- ⁴S. Munnix and M. Schmeits, *Solid State Commun.* **12**, 1087 (1984).
- ⁵R. Alben, M. Blume, H. Krakauer, and L. Schwartz, *Phys. Rev. B* **12**, 4090 (1975).
- ⁶R. Haydock, V. Heine, and M. J. Kelly, *J. Phys. C* **5**, 2845 (1972).
- ⁷D. Weaire and E. P. O'Reilly, *J. Phys. C* **18**, 1401 (1985), and references therein.
- ⁸K. Vos, *J. Phys. C* **10**, 3917 (1977).
- ⁹S. Munnix and M. Schmeits, *Phys. Rev. B* **30**, 2202 (1984).
- ¹⁰Density-functional calculations for single silicon vacancies using the Slater-Koster approach have been carried out by G. A. Barolff and M. Schluter, *Phys. Rev. Lett.* **41** 892 (1978) and J. Bernholc, N. O. Lipari, and S. T. Pantelides, *ibid.* **41**, 895 (1978).
- ¹¹V. E. Heinrich, G. Dresselhaus, and H. J. Zeiger, *Phys. Rev. Lett.* **36**, 1335 (1976).
- ¹²W. Gopel, G. Rockes, and R. Feierabend, *Phys. Rev. B* **28**, 3427 (1983); D. C. Cronmeyer, *Phys. Rev.* **87**, 876 (1952); *ibid.* **113**, 1222 (1959).
- ¹³Similar arguments have been used by M. O. Selme and P. Pecheur, *J. Phys. C* **16**, 2559 (1983) in order to justify a similar model for an oxygen vacancy in SrTiO₃. These authors used the recursion method to investigate the single oxygen vacancy.